UNIVERSITY OF ROCHESTER

SENIOR THESIS

Triggering A Climate Change Dominated "Anthropocene": Is It Common Among Exocivilizations?

Author:
Ethan Savitch

Supervisors:
Professor Adam Frank
Dr. Jonathan Carroll-Nellenback

A thesis submitted to the Department of Physics and Astronomy gaining a full enrichment of the bachelor's degree. Supervised by Professor Adam Frank & Dr. Jonathan Carroll-Nellenback

in the

Department of Physics and Astronomy
University of Rochester

Rochester, New York
2020

This thesis is based on Ethan Savitch et al. (2021). *Triggering A Climate Change Dominated "Anthropocene": Is It Common Among Exocivilizations?* arXiv: 2103.06330 [astro-ph.EP].

Abstract

Triggering A Climate Change Dominated "Anthropocene": Is It Common Among Exocivilizations?

by Ethan Savitch

Bachelor of Science

Professor Adam Frank & Dr. Jonathan Carroll-Nellenback, Supervisors

Department of Physics and Astronomy

We seek to model the coupled evolution of a civilization and their host planet through the era when energy harvesting by the civilization drives the planet into new and adverse climate states. In this way we ask if triggering Anthropocenes of the kind humanity is experiencing might be a generic feature of planet-civilization coevolution. This question has direct consequences for both the study of astrobiology and the sustainability of human civilization. Furthermore, if Anthropocenes prove fatal for some civilizations then they can be considered as one form of a "Great Filter" and are therefore relevant to discussions of the Fermi Paradox. In this study we focus on the effects of energy harvesting via combustion and vary the planet's initial chemistry and orbital radius.

We find that in this context, the most influential parameter dictating a civilization's fate is their host-planets climate sensitivity, which quantifies how global temperatures change as CO_2 is added to the atmosphere. Furthermore, this is in itself a function of the planet's atmospheric CO_2 level, so planets with low levels of CO_2 will have high climate sensitivities and high probabilities of triggering climate change. Using simulations of the coupled nonlinear model combined with semi-analytic treatments, we find that most planets in our initial parameter space experience diminished growth due to climate effects, an event we call a "climate-dominated" Anthropocene.

Contents

Chapter 1

Introduction

Human activity is beginning to drastically alter the state of many of Earths interconnected systems, such as its atmosphere, hydrosphere, biosphere, etc. While there are many measures of our impact on the planet, global warming driven by CO_2 emissions represents the most dramatic (Solomon et al., 2007). Collectively, these planetary changes have been described as a new geological epoch called the Anthropocene (Crutzen, 2002). Recent studies have even shown that 2020 marks the point at which human-made "anthropogenic" mass has exceeded all of Earth's living biomass (Elhacham, Ben-Uri, Grozovski, et al., 2020). Thus, it is of great importance to consider the long-term impacts of the Anthropocene on human civilization.

While the specifics of such impacts are not clear, their consequences have been theorized to be as drastic as full-scale extinction. Also of interest are the requirements needed to successfully enter the Anthropocene and develop a sustainable version of civilization. Such sustainable planetary states were explored in (Frank, Alberti, and Keliedon, 2017). Its even possible that such requirements are nonexistent, so that the Anthropocene represents a "tipping point" at which recovery is futile (Lenton et al., 2008; Kuehn, 2011). Any knowledge that can be gained on the generic features of civilization-planetary co-evolution will be useful in navigating our own version of the Anthropocene.

The ubiquity and severity of Anthropocenes also has large astrobiological implications. Their ubiquity could provide insight into the nature and even existence of technosignatures, i.e. imprints from technology created by an intelligent civilization. While their severity, if fatal for some civilizations, would allow the Anthropocene to be considered as one form of a "Great Filter", making it relevant to discussions of the Fermi Paradox (Carroll-Nellenback et al., 2019).

The aim of this paper is to develop a model that can simulate the coupled relationship between a civilization that harvests energy via combustion and their host planet. Such a model will allow us to gain insight into the fragility of earth-like intelligent civilizations. In addition, it will also allow us to ask if Anthropocenes might be a generic feature of any planet evolving a species that intensively harvests resources for the development of a technological civilization (Haqq-Misra and Baum, 2009; Frank, Alberti, and Keliedon, 2017; Mullan and Haqq-Misra, 2019). We focus our analysis on a specific type of Anthropocene where the main driver for the end of population growth is climate change. We call this a "climate-dominated" Anthropocene.

This paper is a follow-up to Frank et al., 2018, where they investigated the same question by developing an analytic form of the model. Their model consisted of a series of coupled differential equations that were able to roughly model the relationship between energy harvesting civilizations and their host planets. Since this was done by purely analytical means, the aim of this current project is to add a numerical climate model to physically simulate planetary response to an evolving exo-civilization. The model we used is called an Energy Balance Model (EBM), which takes in a variety of planetary inputs and outputs the global temperature, which we take to be representative of the global state (North and Kim, 2017). In this study, the two planetary parameters that we will focus on are orbital distance and partial CO_2 pressure. Since our experience with such coupled relationships is limited to our experiences on Earth, we start by using Earth-like inputs, allowing us to replicate our planets growing population and increasing temperatures. Our paper then asks the question, if we moved Earth to different orbits or changed its partial CO_2 pressure, would we still be experiencing a climate-dominated Anthropocene?

Theoretically, we can reduce our planets temperature by moving it away from the sun in order to decrease the amount of solar radiation reaching us. But, in this case, our ability to produce CO_2 without consequence could end up making the atmosphere toxic, as too much CO_2 can present its own unwanted consequences (Wittmann and Pörtner, 2013). Thus, in setting up our initial conditions we used two key assumptions:

1. The civilization has a biology that requires water to be in its liquid form, this fixes the range of orbital radii by requiring that initial global temperatures be in the range

$$273K < T_0 < 373K$$

2. The civilizations require CO_2 concentrations to be below a certain threshold (Schwieterman et al., 2019; Ramirez, 2020; Catling et al., 2005).

In Schwieterman et al., 2019, they discuss these limited conditions for which complex aerobic life can survive relative to that for microbial life. In doing so they define a Complex Life Habitable Zone (CLHZ) which aims to improve upon the traditional temperature-defined habitable zone. The major difference being that the CLHZ assumes both of our key assumptions, where traditionally only the first assumption is considered. Furthermore, they find that the upper limit for pCO_2 amenable to human life is approximately $5,000$ ppm. This has important implications. For example, the assumption that pCO_2 remain below this produces a habitable zone around our sun that is approximately 65% smaller than that imposed purely by temperature requirements.

The plan of the paper is as follows. In Chapter 2 we develop the coupled model and use Earth-like inputs to calibrate it as well as test its efficacy at modelling technological civilizations. In Chapter 3 we analyze the model to determine its intrinsic timescales, which we further use to develop some dimensionless quantities. We then continue to use these quantities to develop a linearized version of our coupled model, which allows us to derive a dimensionless timescale that could predict the rate that civilizations will collapse. This allows us to identify the solution domains for our model. In Chapter 4 we discuss the results of the full nonlinear coupled model. We first investigate the effect that moving Earth to different orbits or changing its initial CO_2 levels would have on the resulting co-evolution of civilization and host-planet. We then show the results from a full parameter sweep of these two parameters. Finally, we run a suite of models in which the civilizations tolerance for global temperature change is varied. In Chapter 5 we summarize our work, discuss our findings and their implications, and consider possible next steps.

Chapter 2

Developing the Coupled Model

2.1 Overview

Our model consists of three coupled differential equations. They describe the time evolution of global temperature (T), population (N), and partial CO_2 pressure (P).

$$\dot{T} = EBM(P, a) \tag{2.1}$$
$$\dot{N} = f(T, P) \tag{2.2}$$
$$\dot{P} = CN \tag{2.3}$$

Where $\dot{x} = dx/dt$ and a is orbital distance. The first equation is given by our climate model, called an energy balance model (EBM), which will be described in more detail in Section 2.1.1. The second equation is given by a population growth model developed by Adam, Jonathan, and I, which will be described in more detail in Section 2.1.2. The last equation determines how changes in population affect global pCO_2 levels. It says that the rate of increasing pCO_2 in our atmosphere is directly correlated to the global population. Thus, the proportionality constant between the two, denoted C, acts to quantify a civilizations annual, per-capita, carbon footprint.

Our model begins by using the orbital distance (a) and initial partial CO_2 pressure (P_0) as inputs for our climate model (Eq. 2.1) in order to determine the planets initial temperature (T_0). This process will be discussed further in Section 2.1.1. This initial temperature, as well as our planets initial global population (N_0) and atmospheric partial CO_2 pressure (P_0) are then used as inputs for our model of population growth (Eq. 2.2) in order to determine what our planets population would be after some given time period. This method will be described in more detail in Section 2.1.2. After determining this value of population, it is used in conjunction with the planets initial partial CO_2 pressure in order to determine what this value will be after some time Δt, as described by Eq. 2.3. This value of pCO_2 is then inputted back into our energy balance model to repeat the process.

More generally, if Δt is one year, then the algorithm our model follows in order to determine the global temperature, population, and partial CO_2 pressure at year n, as functions of what those values were the year prior is given by:

$$(1)\ T_n = EBM(P_{n-1},\ a)\Delta t + T_{n-1}$$
$$(2)\ N_n = f(T_n,\ P_{n-1})\Delta t + N_{n-1}$$
$$(3)\ P_n = CN_n\Delta t + P_{n-1}$$

2.1.1 Energy Balance Climate Model

Energy balance models (EBM's) approximate planetary temperature by balancing the incoming solar radiation with the outgoing long-wave, terrestrial radiation. Our specific version of the model uses a variety of planetary inputs, such as pCO_2 levels, orbital semi-major axis, planetary albedo, orbital eccentricity, etc. The code is 1-D in that it models climate as a function of latitude. The program then discretizes global temperatures into these bands in order to model our latitudinal heat transport as diffusion according to the equation

$$C_v \frac{dT(\theta, t)}{dt} = \psi(1 - A) - I + \nabla \cdot (\kappa \nabla T(\theta, t)) \tag{2.4}$$

Where C_v is the effective heat capacity of the surface and the atmosphere, T is global temperature, θ is latitude, ψ is the solar flux, A is the planetary albedo as a function of both temperature and partial CO_2 pressure, I is the outgoing infrared radiation, and κ is the diffusive parameter. For our purposes we averaged over all latitudinal bands in order to find an average global temperature.

Our version of the model incorporates the effect of carbon dioxide concentrations by making both I and A functions of temperature and partial CO_2 pressure. The code we used was originally developed by Darren Williams in Williams and Kasting, 1997. It was then modified by Jacob Haqq-Misra, who used it most recently in Fairen, Haqq-Misra, and P., 2012. This version of the model is publicly available on GitHub at `https://github.com/BlueMarbleSpace/hextor/releases/tag/1.2.2`.

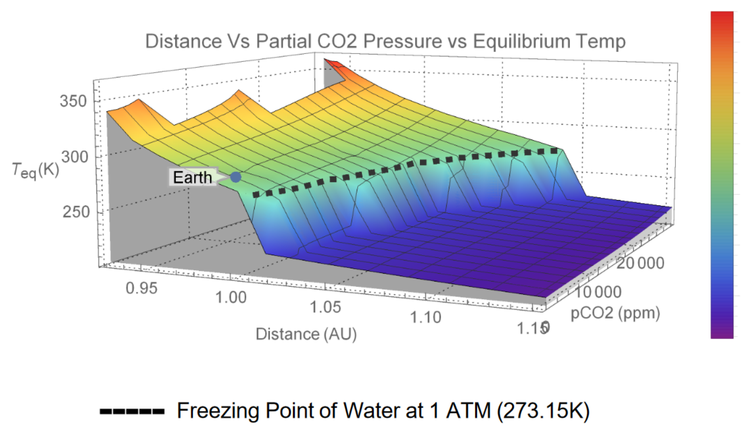

Figure 2.1: Surface plot of our solar systems Habitable Zone, calculated with the EBM given by Eq. (2.4). The blue dot marks the location of our planet, where the temperature was given by our pre-Anthropocene value of approximately 287.09K

2.1.2 Population Model

The differential equation governing population growth initially acts like exponential growth, with an initial per-capita growth rate, R_0, defined as the difference between the per-capita birth (A_0) and death (B_0) rates.

$$R_0 \equiv A_0 - B_0 = \left. \frac{1}{N} \frac{dN}{dt} \right|_{t=0}$$

This acts to represent our civilizations growth rate prior to the Anthropocene, and is thus called the natural growth rate. We allow the growth rate to vary with time in order to incorporate the effects of technological advancements and climate change. In our model we assume that a civilizations technological abilities are correlated with their production of combustion byproducts. Furthermore, as their technological abilities increase, so does their ability to produce offspring. Thus, we define an enhanced growth term which acts to raise our civilizations net growth rate as the amount of CO_2 in the atmosphere increases from its initial value.

$$R_+ = R_0 \left(1 + \frac{P - P_0}{\Delta P}\right)$$

Where ΔP is a normalization constant that roughly corresponds to the amount of pCO_2 that needs to be generate by a civilization in order to double their growth rate. As technology increases the corresponding feedback raises global temperatures. Thus, we define a diminished growth term to lower the net growth rate as planetary temperatures increase from their initial values.

$$R_- = R_0 \left(\frac{T - T_0}{\Delta T} \right)^2$$

Where ΔT is a normalization constant that describes the range of temperatures amenable to a civilizations health. Thus, this quantity is called the civilizations "temperature tolerance". This term can refer to either a persons biology or the civilization as a whole. The final governing equation for population is

$$\frac{dN}{dt} = min[NR_+,\ R_0(N_{max} - N)] - NR_-$$

The min function in the above expression was used to introduce a carrying capacity (N_{max}) into the systems dynamics while avoiding any nonlinear dependencies on population. The carrying capacity acts to smoothly decrease the civilizations growth rate as they approach their maximum population. It ensures that the civilizations don't grow to levels that are unrealistic based purely on food production capabilities. Putting it all together gives

$$\begin{aligned} \dot{N} = f(T,P) &= \min\left[NR_0 \left(1 + \frac{P - P_0}{\Delta P} \right),\ R_0(N_{max} - N) \right] - NR_0 \left(\frac{T - T_0}{\Delta T} \right)^2 \\ &= R_0 N \left[\min\left(1 + \frac{P - P_0}{\Delta P},\ \frac{N_{max}}{N} - 1 \right) - \left(\frac{T - T_0}{\Delta T} \right)^2 \right] \end{aligned}$$

2.2 Testing the Model

Table 2.1: Earth-Like Inputs for Coupled Model

Parameter	Description	Earth Value
N_{max}	Carrying Capacity	20 billion
$R_0 = A_0 - B_0$	Initial Birth Coeff.	0.005 yr^{-1}
ΔT	Population Temp Tolerance	$5K$
ΔP	Technology Birth Benefit	30 ppm
C	per capita CO_2 generation	$2.75 \times 10^{-4} \frac{ppm}{10^6 ppl * yr}$

In order to provide both a test and a calibration of our model we run it using Earth-like inputs. We allow the model to start at $t_0 = 1820\ CE$, when the global population was $N_0 = 1.29\ Billion$ and the global pCO_2 levels were around $P_0 = 284\ ppm$. The rest of the input variables are shown in Table 2.1. The resulting evolution of temperature, population, and growth rate is shown in Figure 2.2. Furthermore, see Figure 2.3 to see a comparison between some of our models free parameters and their analogous values on Earth.

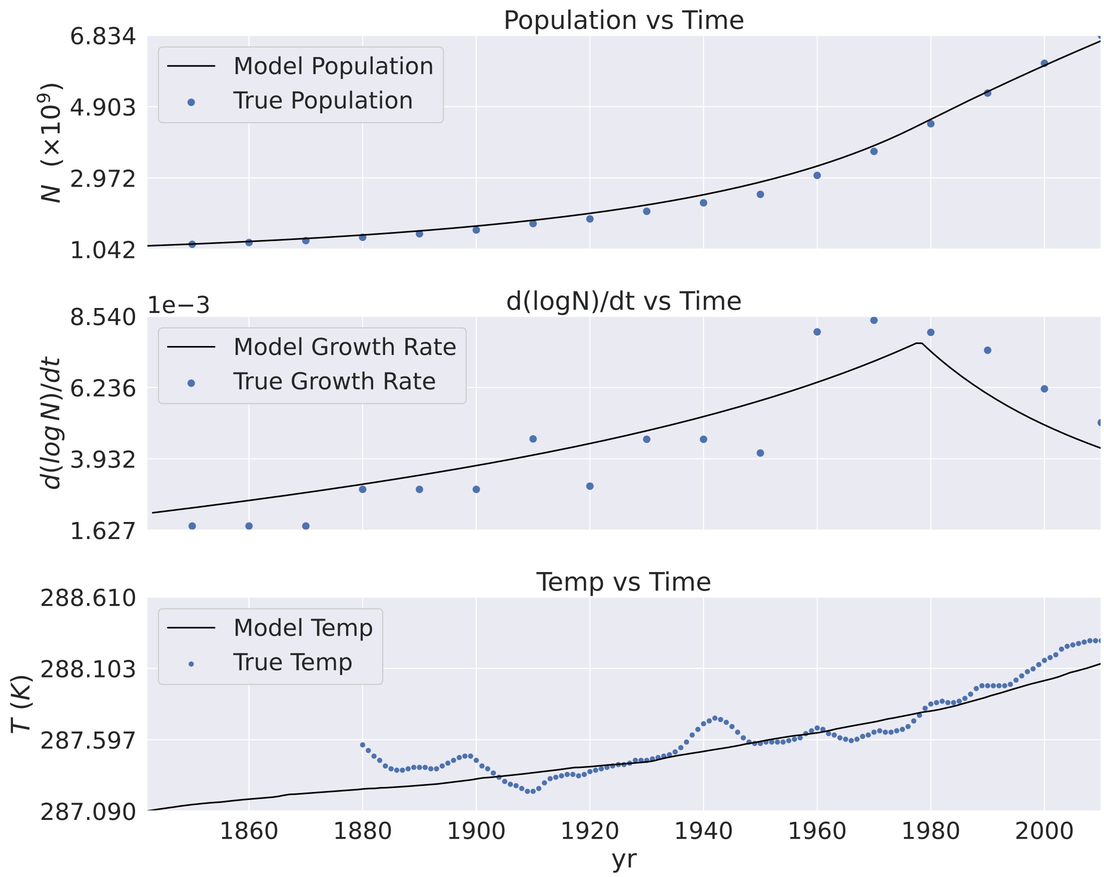

Figure 2.2: The model results are the solid black line and global data is represented by the blue dotted line. As can be seen, the model does a pretty good job of tracking the rise in population, growth rate, and temperature during the last two centuries.

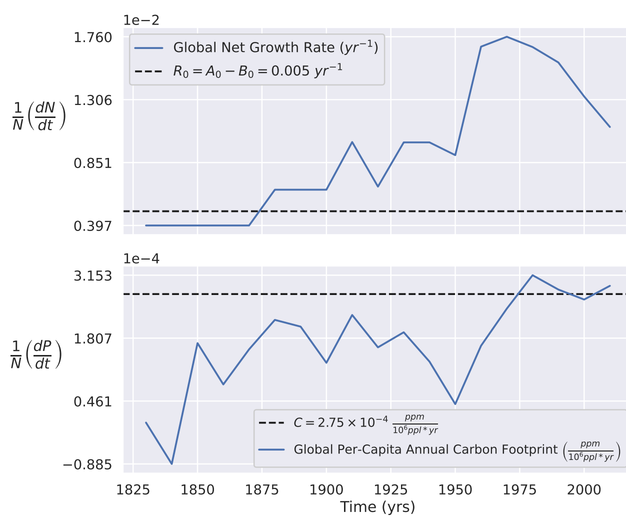

Figure 2.3: The birth rate A_0 was fixed by the assumption that the average time between births was approximately 25 years. The death rate B_0 was then adjusted to tune the population part of our model. The resulting natural growth rate is approximately what it was on Earth prior to the Anthropocene, shown in the top plot as the black dotted line. Finally, we adjusted C in order to match our climates response to population growth, shown as the dotted line in the bottom plot. The resulting value is approximately equal to its current value on Earth.

Chapter 3

Analyzing the Coupled Model

3.1 Climate Sensitivity

In order to derive a timescale for climate change, we first need a way to quantify how changes in pCO_2 affect global temperatures. This relationship can be approximated by assuming that temperature has a simple logarithmic dependence on pCO_2 (Huang and Bani Shahabadi, 2014)

$$T \approx T_0 + \Delta T_F \log(P/P_0) \tag{3.1}$$

Where T_0/P_0 are the initial values of global temperature and partial CO_2 pressure. Taking the derivative of this yields one of the most influential quantities that determines civilization-planet coevolution, called 'climate sensitity', traditionally defined by the rate at which global temperatures change proportional to pCO_2.

$$\frac{dT}{dP} = \frac{\Delta T_F}{P} = \frac{\Delta T_F}{P_0} e^{-\left(\frac{T-T_0}{\Delta T_F}\right)} \equiv De^{-\left(\frac{T-T_0}{\Delta T_F}\right)} = \textit{Climate Sensitivity} \tag{3.2}$$

Thus, ΔT_F acts to quantify the change in temperature required for the climate sensitivity to drop by a factor of e, and is approximately $4K$ for Earth (IPCC, 2014). Furthermore, we have defined

$$D \equiv \frac{\Delta T_F}{P_0} = \left.\frac{dT}{dP}\right|_{P=P_0} = \textit{Initial Climate Sensitivity} \tag{3.3}$$

As a result, it follows that

$$P_0 = \frac{\Delta T_F}{dT/dP|_{P_0}} = \textit{Initial } pCO_2$$

This relationship allows us to bifurcate our model into two classes of solutions.

(a) Low P_0

- High Initial Climate Sensitivity $(dT/dP|_{P_0})$ means that the initial planetary state will be very unstable against small perturbations in pCO_2.
- Low ΔT_F means that only a small change in temperature is needed to dramatically reduce this climate sensitivity.
- We expect civilizations on such planets to be at a high risk for a climate-dominated Anthropocene as defined in Chapter 1.

(b) High P_0

- Low Initial Climate Sensitivity $(dT/dP|_{P_0})$ means that the initial planetary state will be less sensitive to small perturbations in pCO_2.
- High ΔT_F means that a large amount of pCO_2 must be generated by a civilization in order to reduce this climate sensitivity further.

- We expect civilizations on such planets to be at a low risk for a climate-dominated Anthropocene, yet a high risk for overpopulation or CO_2 poisoning.

3.2 Intrinsic Timescales

In analyzing the model we see that their are three intrinsic timescales. The population dynamics are dictated by the net growth rate, as discussed in Section 2.1.2. Thus, the initial value of this is what determines our first relevant timescale, that for population growth.

$$\boxed{t_G = \frac{1}{R_0} = \textit{Timescale for Population Growth}}$$

We can also define a timescale to quantify the rate of a civilizations technological advancements.

$$\boxed{t_T = \frac{\Delta P}{CN_{max}} = \textit{Timescale for Technological Advancements}}$$

Finally, using our approximations for climate sensitivity given in Section 3.1, our last timescale quantifies how climates respond to evolving civilizations.

$$\boxed{t_C = \frac{\Delta T}{CN_{max}D} = \textit{Timescale for Climate Change}}$$

The temperature tolerance (ΔT) appears as it dictates the timescale for climate to be driven out of its "safe operating zone".

3.3 Dimensionless Quantities

We can continue by using the three timescales derived above, in Section 3.2, to define some dimensionless quantities. First, we define γ to be the ratio of the population growth timescale to the climate change timescale.

$$\boxed{\gamma = \frac{t_G}{t_C} = \frac{DCN_{max}}{R_0 \Delta T}}$$

This acts to quantify a civilizations risk of having an Anthropocene in an analogous way to how we used P_0 in Section 3.1. In fact, the two cases discussed in that section directly correlate with the cases of high and low γ. As shown in that section, if P_0 is very low, then the initial climate sensitivity (D) will be very high (Eq. 3.3). Thus, the case of very low initial partial CO_2 pressure (P_0) correlates to that for very high γ. Similarly, very high P_0 will result in a very low γ.

If $\gamma = 1$, then the rate of climate change and population growth is equivalent. The value of the carrying capacity required to accomplish this is then representative of the number of people required to force the climate out of equilibrium in a single growth timescale. We call this quantity the "Anthropogenic Population", defined like

$$N_A \equiv \frac{N_{max}}{\gamma} = \frac{R_0 \Delta T}{DC}$$

Furthermore, we can define another dimensionless quantity, denoted θ, by dividing the climate timescale by the technological timescale

$$\boxed{\theta = \frac{t_C}{t_T} = \frac{\Delta T}{D\Delta P}}$$

This then acts to quantify how much technology can enhance population growth as the civilization is in the process of destroying their environment, i.e. as global temperatures change by ΔT. It follows that multiplying this by γ give us another parameter, defined as the ratio between the timescale for population growth to that for technology to advance.

$$\boxed{\beta \equiv \theta\gamma = \frac{t_G}{t_T} = \frac{CN_{max}}{R_0\Delta P}}$$

Since this is independent of D, it acts to quantify the extent to which CO_2 production increases net growth rates under the assumption that the civilization is already at its carrying capacity. This can be used to define a technological civilization, which is of interest as these are the type of civilizations we are interested in for this paper. We say that a civilization is 'technological' if and only if they have $\beta > 1$, meaning that their timescales for technological advancements are shorter than that for their population to grow.

With our three timescales we would expect our coupled model to have six domains of behavior, but the requirement that $\beta > 1$ eliminates half of these.

(1) Climate-dominated Anthropocene ($\gamma > 1$)

- $\cancel{t_T > t_G > t_C \implies \theta < 1, \beta < 1}$
- $t_G > t_C > t_T \implies \theta > 1, \beta > 1$ ✓
- $t_G > t_T > t_C \implies \theta < 1, \beta > 1$ ✓

(2) Overpopulation ($\gamma < 1$)

- $\cancel{t_T > t_C > t_G \implies \theta < 1, \beta < 1}$
- $t_C > t_G > t_T \implies \theta > 1, \beta > 1$ ✓
- $\cancel{t_C > t_T > t_G \implies \theta > 1, \beta < 1}$

Three domains remain. In summary, technological civilizations in our model either experience a climate-dominated Anthropocene or overpopulate their planet. If they are experiencing an Anthropocene then their technological abilities will dictate the dynamics of their evolution and eventual collapse. This will be discussed in more detail in Section 3.5.

A last dimensionless quantity arises from our multiple definitions of normalized temperature change. The temperature tolerance, ΔT, is defined to be the temperature change required to decrease net growth rates, thus is focused on the civilizations biology. In contrast, ΔT_F is the temperature change needed to change the climate sensitivity dT/dP, thus is focused on the civilizations environment. The ratio of these two then tells us the number of e-foldings it takes for climate sensitivity to drop as global temperatures change by ΔT.

$$\boxed{\alpha \equiv \frac{\Delta T}{\Delta T_F}}$$

See Section 3.4.1 for more information on its affect on the models.

3.4 Dimensionless Model

Our complete coupled model is given by the three equations

$$\frac{dP}{dt} = CN \tag{3.4}$$

$$\frac{dT}{dt} = EBM(P, a) \tag{3.5}$$

$$\frac{dN}{dt} = R_0 N \left[\min\left(1 + \frac{P - P_0}{\Delta P},\ \frac{N_{max}}{N} - 1\right) - \left(\frac{T - T_0}{\Delta T}\right)^2 \right] \tag{3.6}$$

Before introducing any dimensionless quantities, we can combine our equations governing temperature and pCO_2 change by applying the approximation discussed in Section 3.1 given by Eq. 3.2.

$$\frac{dT}{dt} = \frac{dT}{dP}\frac{dP}{dt} = \left(De^{-\frac{T-T_0}{\Delta T_F}}\right)(CN) = CNDe^{-\frac{T-T_0}{\Delta T_F}} \tag{3.7}$$

Furthermore, we can remove the pCO_2 dependence on our equation governing population growth by employing the approximation given by Eq. 3.1. This results in

$$\frac{dN}{dt} = R_0 N \left[\min\left(1 + \frac{P_0}{\Delta P}\left[e^{\frac{T-T_0}{\Delta T_f}} - 1\right],\ \frac{N_{max}}{N} - 1\right) - \left(\frac{T - T_0}{\Delta T}\right)^2 \right] \tag{3.8}$$

Now in order to derive the complete dimensionless model, we need some more dimensionless quantities, summarized in Table 3.1. With these definitions, we can divide Eq. 3.7 by $R_0 \Delta T$ and Eq. 3.8 by $R_0 N_{max}$ to arrive at our dimensionless model.

$$\frac{d\eta}{d\tau} = \min\left[\eta\left(1 + \frac{\theta}{\alpha}\left(e^{\alpha\epsilon} - 1\right)\right), 1 - \eta\right] - \eta\epsilon^2 \tag{3.9}$$

$$\frac{d\epsilon}{d\tau} = \gamma\eta e^{-\alpha\epsilon} \tag{3.10}$$

Table 3.1: Dimensionless Model Quantities

Var	Definition	Description
η	N/N_{max}	Normalized population
τ	$R_0 t$	Normalized time
ϵ	$(T - T_0)/\Delta T$	Normalized temperature
θ	$\Delta T/(D\Delta P)$	Normalized Birth rate acceleration
γ	$(DCN_{\text{max}})/(R_0 \Delta T)$	Normalized forcing
α	$\Delta T/\Delta T_F$	Ratio of temperature change to affect biology to temperature change to affect climate sensitivity
β	(CN_{max}) / $(R_0 \Delta P)$	Increase in birth rate after burning sufficient CO_2 to change temperature by ΔT

3.4.1 Role of α

It is worth considering the role that α plays in our model. As shown above, we have defined it like

$$\alpha = \frac{\Delta T}{\Delta T_F} = \frac{\textit{Temperature Change to Affect Biology}}{\textit{Temperature Change to Affect Climate Sensitivity } (dT/dP)}$$

As a result, if $\alpha \gg 1$, then $\Delta T_F \ll \Delta T$. In this case we know that climate change will have a greater impact on climate sensitivity then it will have on the growth rate. Since increasing temperatures reduce both quantities, we know that climate change will reduce the climate sensitivity before reducing the net growth rates for civilizations with high α. Figure 3.1 shows runs with $\gamma = 10$, $\theta = 1$ and $\alpha = 0,\ 1,\ \&\ 2$.

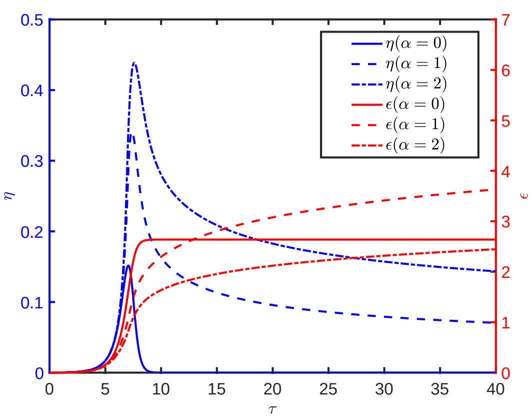

Figure 3.1: Trajectories for different values of α. As compared to the run with $\alpha = 0$, the models with higher α take longer for their death rates to overtake their birth rates, which raises the peak population while delaying the time for it to be reached. Furthermore, the higher α means that temperature changes lead to a greater reduction in climate sensitivity (dT/dP), which has the effect of softening the decline.

3.5 Dimensionless Timescales (Low α Limit)

In the limit of low α, Eqs. 3.9 and 3.10 reduce to

$$\dot{\eta} = \min\left[\eta(1+\theta\epsilon), 1-\eta\right] - \eta\epsilon^2 = d\eta/d\tau$$
$$\dot{\epsilon} = \gamma\eta = d\epsilon/d\tau$$

It is of interest to note that the first term in the min function, $\eta(1+\theta\epsilon)$, represents the civilizations technologically-enhanced growth rate. While the second term, $1-\eta$, places an upper limit on how much technology can boost such rates by enforcing a maximum growth rate, thus acts analogously to the carrying capacity in the full nonlinear model. We find that the dimensionless time for civilizations to collapse after reaching their peak population is

$$\tau_{\text{coll}} = \begin{cases} 1/\gamma & \gamma \ll 1, \theta \gg 1 \\ 1/\theta & \gamma \gg 1, \theta \gg 1 \\ 1/\sqrt{2} & \gamma \gg 1, \theta \ll 1 \end{cases} \tag{3.11}$$

Qualitatively, the behavior of our models in these three regions of parameter space can be summarized as follows

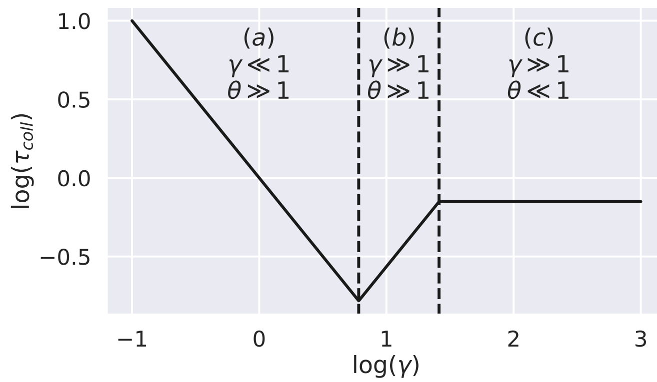

Figure 3.2: The two black dotted lines divide the plot into the three regions discussed above. The leftmost region (a) has $\gamma \ll 1$, and is independent of θ. The middle region (b), is defined by $\gamma \gg 1, \theta \gg 1$. The rightmost region (c), is defined by $\gamma \gg 1, \theta \ll 1$.

(a) $\gamma \ll 1, \theta \gg 1 \quad (t_C > t_G > t_T)$

- In this region, populations grow faster than temperatures increase, so civilizations will reach their carrying capacities before their changing climate begins to increase their death rates.
- As a result, their collapse rate is dictated by the rate of climate change, which we found in Section 3.2
$$\tau_{\text{coll}} = R_0 t_C = \frac{1}{\gamma}$$

(b) $\gamma \gg 1, \theta \gg 1 \quad (t_G > t_C > t_T)$

- In this region, the timescale for climate change is less than that for population growth, but greater than that for technological advancements
- Thus, civilizations will have enough time to gain technological abilities capable of increasing their birth rates, but will not be able to reach their carrying capacity with this enhanced growth rate.
- As a result, civilizations will enter the Anthropocene with a higher than natural, "technologically-enhanced" growth rate, which as a result leads to a higher than natural, "technologically-enhanced" collapse rate

$$\tau_{\text{coll}} = \frac{1}{\theta} = \frac{\gamma}{\beta}$$

(c) $\gamma \gg 1, \theta \ll 1 \quad (t_G > t_T > t_C)$

- In this region, the timescale for climate change is less than that for population growth and technological advancements
- Thus, civilizations will begin to fall before they have had enough time to substantially increase their population or technological capabilities.
- As a result, all civilizations in this region will enter the Anthropocene with their "natural" growth rate (R_0), thus will also collapse with approximately the same "natural" collapse rate, which we find to be

$$\tau_{\text{coll}} = \frac{1}{\sqrt{2}}$$

Equation 3.11 was graphed by rewriting it in the following form

$$\tau_{\text{coll}} = \max\left[\frac{1}{\gamma}, \frac{1}{\max(\sqrt{2}, \beta/\gamma)}\right] \tag{3.12}$$

Where $\beta = \theta\gamma$ is assumed to be constant across all the models at approximately 36.67. The full derivation/explanation for how we found Eqs. 3.11 and 3.12 is shown in Appendix A.

Chapter 4

Exploring the Coupled Model

4.1 Constant Temperature/Composition Models

We now return to the complete nonlinear coupled model discussed in Chapter 2. As mentioned in the introduction, the motivation behind this study is to investigate the fragility of earth-like intelligent civilizations. Specifically, we were interested in how the co-evolution of such civilizations and their host planets depends on various initial conditions. The two parameters that we focused on were the orbital distance of the planet (a) and its initial partial CO_2 pressure $(P_0 = pCO_{2,0})$. The effect of these parameters on the model are not independent, as they both affect the planets climate sensitivity (dT/dP), as discussed in Section 3.1.

In order to explore our models dependencies on these parameters, we ran two experiments. The first of these we called "constant composition". These keep initial pCO_2 constant and allow the initial (equilibrium) planetary temperature, T_0, to vary as we change the orbital distance (a). Using $T_0 = 287K$ as our fiducial value, we ran four additional models with temperatures evenly spaced above and below T_0 in steps of $6K$. This spacing was chosen in order to have all models safely within the classically defined habitable zone, so that water on the surface remains in its liquid form ($273K < T_0 < 373K$). In Figure 4.1 we show the location of the models in the (a, T_0) plane. This representation is important because we will later overlay contours of various quantities such as γ and the collapse time (τ_{coll}) when we run a larger array of models that sweep across (a, T_0) space.

The second set of experiments are "constant temperature" models. We varied initial pCO_2 to keep $T_0 = 287K$. Five models were run centered on Earth's pre-Anthropocene pCO_2 level $(P_0 = 284\,ppm)$ with two below and three above each spaced by $log(pCO_2) = 0.7$. The highest, $P_0 \approx 28,000$ ppm, was meant to illustrate the evolution of a system with CO_2 concentrations beyond what animal life on Earth can tolerate (Schwieterman et al., 2019).

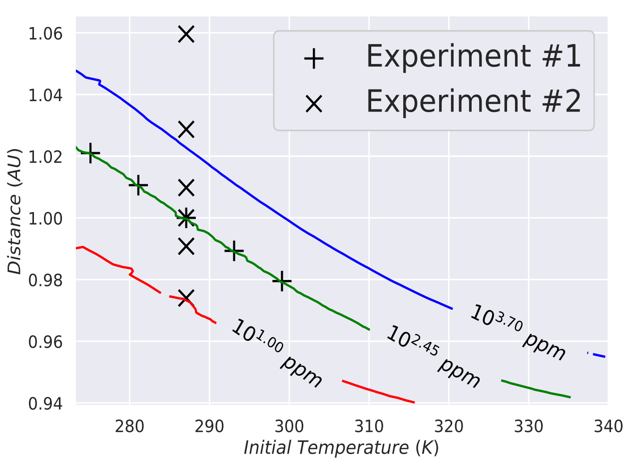

Figure 4.1: Experiment #1: Constant Composition was defined by constant levels of $pCO_2 = 284\ ppm$, and is denoted by the pluses (+). Experiment #2: Constant Temperature was defined by constant equilibrium temperature $T_{eq} = 287.09K$, and is denoted by the crosses ($\times$). The two experiments intersect at Earth when $pCO_2 = 284\ ppm$ and $T_{eq} = 287.09$.

In Figure 4.2 we show all trajectories for both experiments. The upper panel shows results from constant initial composition models while the lower panel shows those for constant initial temperature models. The similarities and differences both within and between the models offers insight into the dynamics and its relationship to our dimensionless parameters. For example, the value of γ can be seen to uniquely determine the resulting evolution of population. Furthermore, the upper panel shows that models with constant pCO_2 yet different orbital radii and initial temperatures will share the same γ. The reasoning for this will be discussed in Section 4.2.

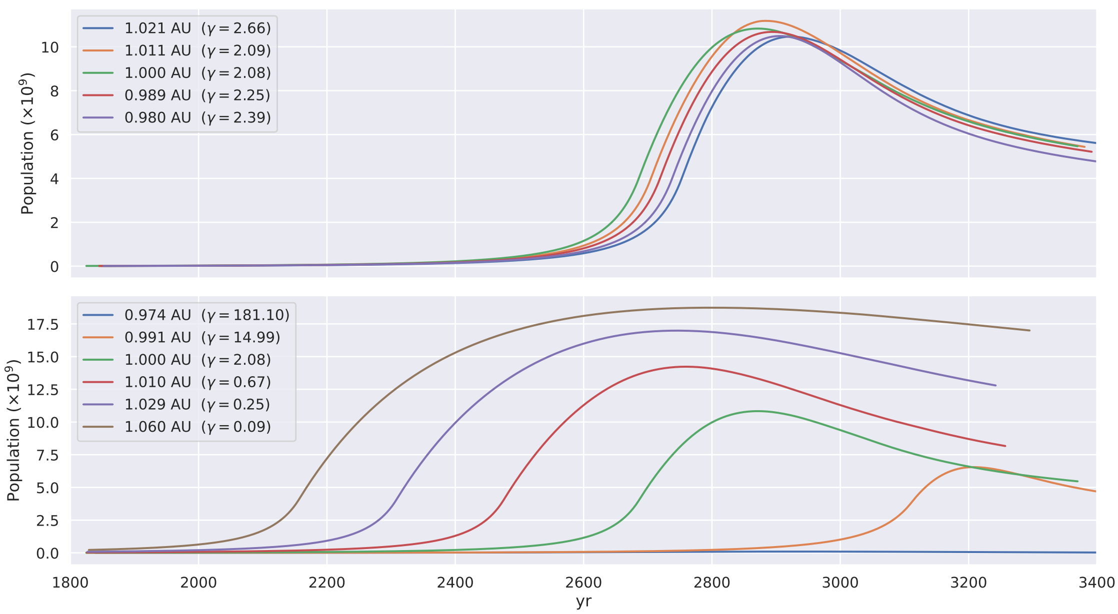

Figure 4.2: The top plot shows the trajectories for Experiment #1: Constant Composition, defined by constant levels of initial pCO_2 ($P_0 = 284\ ppm$). The bottom plot shows the trajectories for Experiment #2, defined by constant initial global temperatures ($T_0 = 287.09K$). The most influential quantity for the co-evolution of intelligent civilizations and their planets is the climate sensitivity (dT/dP), which is a function of pCO_2. The initial value of pCO_2 was found in order to make any given distance have any given temperature. Thus, this value of initial pCO_2 principally determines the resulting co-evolution. This is why the trajectories for Experiment #1 are very similar, as they all have approximately equal initial levels of pCO_2. In contrast, the trajectories in the bottom plot all have the same temperature, but different distance. As a result, these models also have different levels of initial pCO_2, resulting in different climate sensitivities. This is why the trajectories in this plot are much more diverse.

4.2 Parameter Sweeps of Initial Temperatures and Orbital Radii

To explore the broad dependence on initial conditions we next choose 100 different distances (a) and initial temperatures (T_0) for the models. The results of this parameter sweep are shown as a grid of contour plots in Figure 4.3. The left column of the plots show quantities taken from the full numerical models, while the right column shows the corresponding analytical quantities.

In the top left we present contours and color mapping of the initial atmospheric composition, $\log(P_0) = log(pCO_{2,0})$, for all the runs. This was calculated using only the uncoupled energy balance model. Note that we exclude models with $\log(P_0) > 3.7$ as being outside the CLHZ (Schwieterman et al., 2019), as discussed in Chapter 1.

The top right panel in Figure 4.3 presents effective γ, defined like $\gamma_{\text{eff}} \equiv \gamma e^{-\alpha}$, as will be discussed in Appendix B, where $\alpha = \Delta T/\Delta T_F$ and

$$\gamma = \frac{DCN_{max}}{R_0 \Delta T}$$

Since all of our models shared earth-like parameters, differing only by $T_0/P_0/N_0$, the only term in γ that differs between them is D. Thus, as discussed in Section 3.1, it follows that

$$\gamma \propto D \equiv \left.\frac{dT}{dP}\right|_{P_0} = \frac{\Delta T_F}{P_0} \tag{4.1}$$

As a result, γ is principally determined by the initial value of the climate sensitivity, $dT/dP|_{P_0}$, which as shown above is inversely proportional to the initial partial CO_2 pressure (P_0). It follows that P_0, shown in the top-left panel of Figure 4.3, uniquely determines what γ is. As a result, the contour lines of initial P_0 also correspond to contour lines of γ_{eff}. Recall that even models with with γ slightly less than 1 can still have their development hindered by environment impacts. Thus, we find that most civilizations in the CLHZ (as defined in Chapter 1) will be at risk for a climate-dominated Anthropocene.

The middle row describes the population dynamics for the civilizations and focuses on parameters associated with population growth. The left column presents the numerically measured percentage of the carrying capacity that each civilization reached, N_{peak}/N_{max}. Note that all models in the parameter sweep began with a carrying capacity of $N_{max} =$ 20 billion. We see that only the outermost orbits at each initial temperature are able to rise to their carrying capacity before increasing temperatures significantly increase death rates and halt population growth. The right column shows the analytic predictions of the similar quantity, N_A, defined in Section 3.3 as the number of people required to force the climate out of equilibrium in a single growth timescale ($t_G = 1/R_0$).

Finally, the last row of plots considers what happens after the population reaches its peak, $N = N_{peak}$. On the left we show the time for populations to decline by 20% from their peak. Here we see most of the models experience a decline on timescales of a few centuries while initially hotter worlds on inner orbits can have declines over decades. The analytically derived collapse timescale, τ_{coll}, is shown as the plot in the lower right. Once again we see timescales of order decades to a few centuries associated with significant population decline. It is of interest that τ_{coll} shows the "valley" feature at intermediate orbital distances where it falls and then rises again as one moves outward in orbital distance along a line of constant T_0. This is as expected, and the reasoning is explained in Section 3.5.

4.3 Dependence of Civilization Temperature Tolerance (ΔT)

All the models discussed in the last section used a constant value for the civilization's temperature tolerance, $\Delta T = 5K$. This parameter defines the range of temperatures amenable to a civilizations health, and is intended to capture any biological/sociological aspects of the pop-planet co-evolution. Thus, in this section we vary ΔT to investigate its effect on

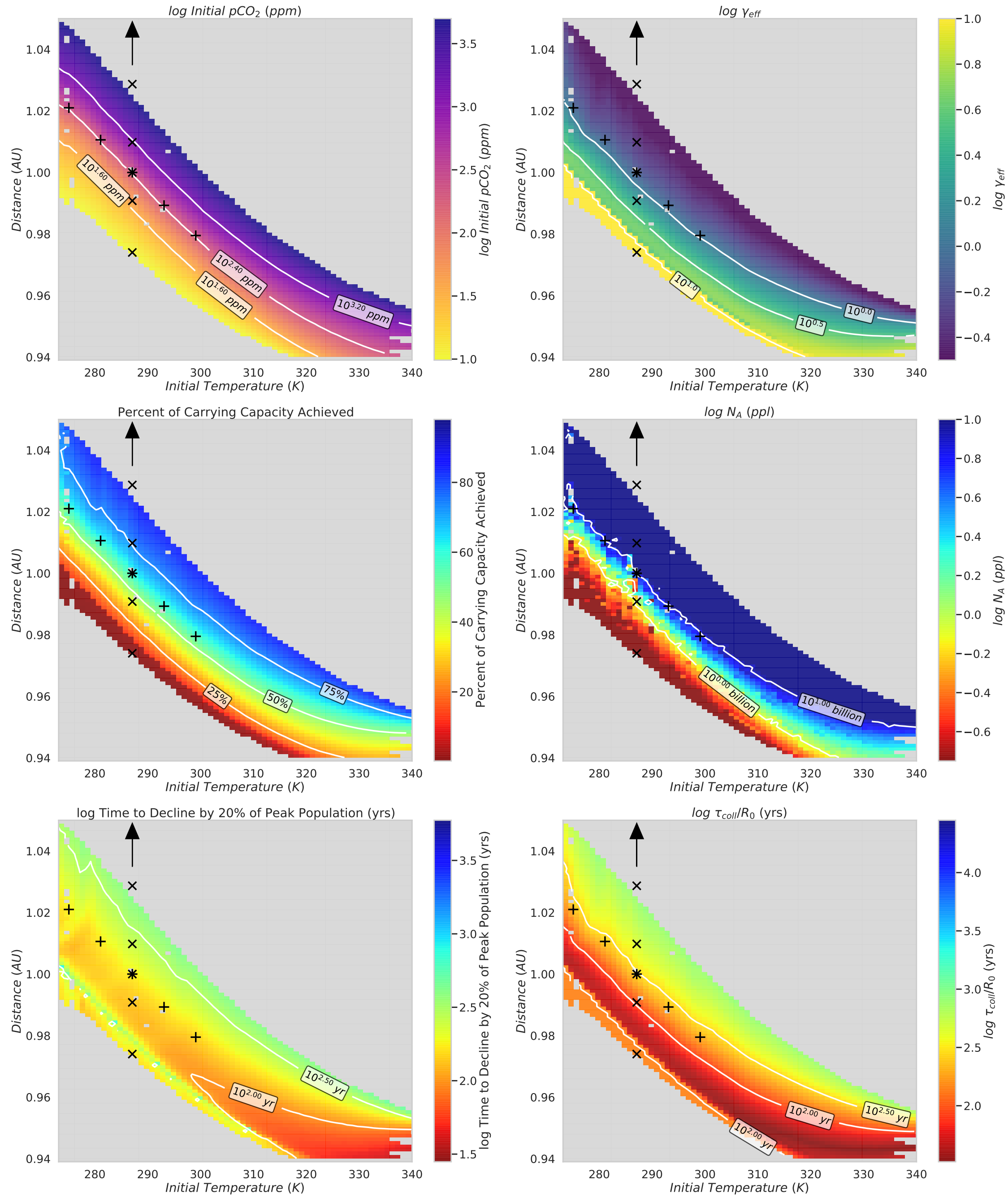

Figure 4.3: The plots on the left hand side show numerically calculated quantities, while the plots on the right hand side show analytically derived quantities. The top row shows values calculated with the uncoupled energy balance model. The middle row shows quantities related to the populations growth. The bottom row shows timescales related to the populations collapse. The bottom left of the plots are grey because of limitations imposed by the EBM. The top right part of the plots are grey because the value of pCO_2 required there was greater than $5,000\ ppm$, a level deemed uninhabitable for long-term habitability by intelligent civilizations (Schwieterman et al., 2019). The black arrow points to the location of the experiment that we ran in the 'danger zone'.

the models outcomes. We accomplish this by repeating the parameter sweep discussed in the last section for $\Delta T = 0.5K$, $1K$, $2.5K$, and $10K$. The results are summarized in Figure 4.4, where we show the marginal probability distributions for both γ_{eff} and the time for civilizations to decline. These are represented as "violin plots", which show the probably distribution of each for all values of ΔT, along with their median values and first moments.

Note that the median values for the collapse times increase with values of ΔT. This is to be expected as the larger range of tolerated temperatures leads to a higher probability for civilizations to reach their carrying capacity before increasing temperatures can cause them to collapse. The distributions of γ_{eff} reflect this by showing how increasing temperature tolerances decrease γ (see Section 3.3).

We also show data for the models as a scatter plot of γ_{eff} versus decline time in Figure 4.5. On the x and y axis we show corresponding marginal probability distributions for γ_{eff} and the decline time. These are shown as a kernel density estimation graph such that the area under each curve is normalized to one. Shown as the solid black line is our analytically derived collapse time, given by Equation 3.12. It can be seen that our analytic approximation reproduces the necessary features that arise in our numerical runs. The two vertical dashed lines divide the graph into three regions, as discussed in Section 3.5.

In summary, the leftmost region corresponds to low γ and high θ. This region results largely in overpopulation, which is the reason behind the long decline times. The middle region corresponds to both high γ and high θ, where technology is able to accelerate birth rates, but eventually ends up contributing to an increased death rate and a shortened decline time. The rightmost region corresponds to a high γ and a low θ, where climate changes on a faster timescale then both technology and population growth. Thus, in this region, civilizations experience climate change before they experience any growth benefits due to technology. This means that these civilizations reach only a tiny fraction of their carrying capacity before they begin to decline.

Also, we note that in Figure 4.5 the distribution for $\Delta T = 1K$ seems to peak higher than $\Delta T = 0.5K$. This occurs because many of the models with $\Delta T = 0.5K$ are in the 'valley' of our collapse time, and the marginal distribution is a projection onto the y-axis. This can also be seen as the large shoulder protruding in the distribution of collapse times for $\Delta T = 0.5K$. Despite this, the violin plots shown in Figure 4.4 confirm that the median time to decline for $\Delta T = 0.5K$ is less than that for $\Delta T = 1K$

The most important takeaway from these results is that an ever increasing share of the models experience climate-dominated Anthropocenes as ΔT decreases. For $\Delta T < 5K$, most models experience rapid population declines. Even for $\Delta T = 10K$, the average decline time was 384.04 years and 22.2% of models had decline times less than 200 years.

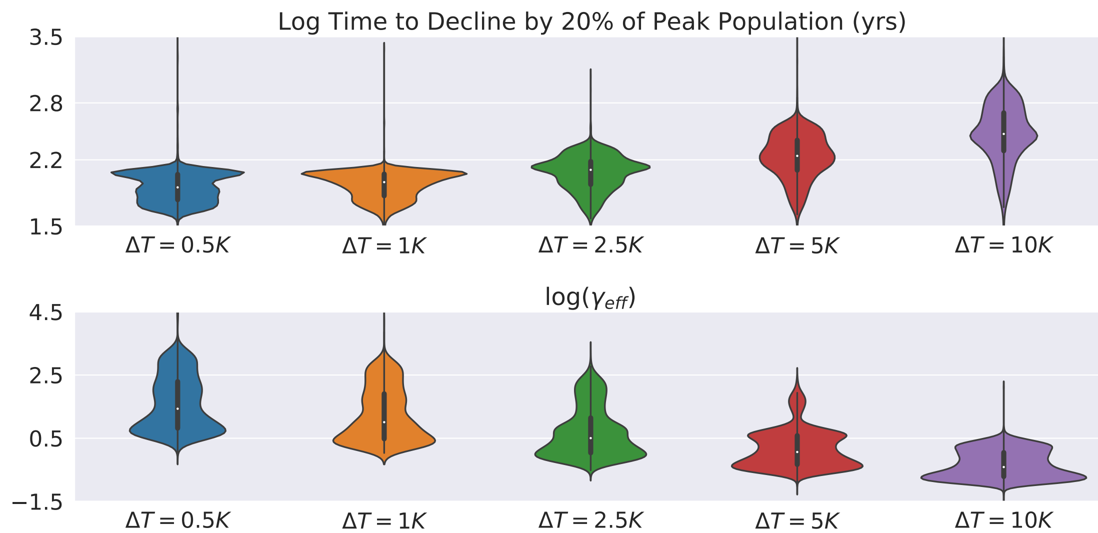

Figure 4.4: This figure shows a box plot of the marginal distributions shown in Figure 4.5. The white dot represents the median value. The box's lower bound corresponds to the median of the lower half of the data-set, while the box's upper bound is the median of the upper half of the data-set. It is of interest to note how increasing the population-temperature sensitivity parameter (ΔT) results in a steadily decreasing γ_{eff} and a steadily increasing time for the population to decline.

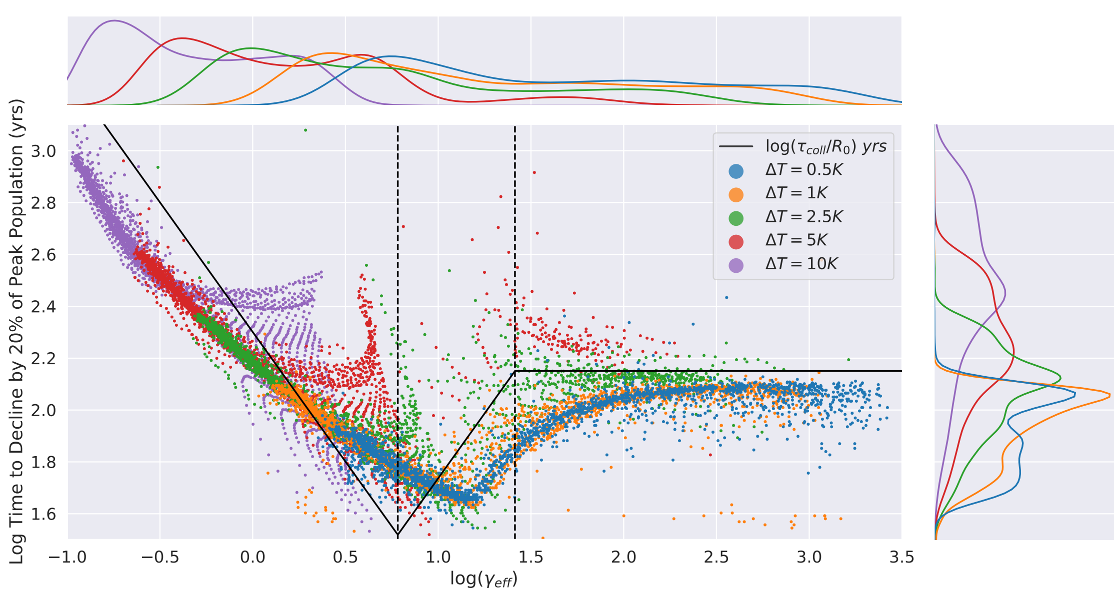

Figure 4.5: Shown above is a scatter plot of γ versus the time for civilizations to decline by 20% of the their peak population. The solid black line shows our analytically derived collapse time, given by Eq. 3.12. The colors represent different values of our temperature tolerance ΔT. The black dashed lines divide the graph into three regions, as discussed in Section 3.5.

Chapter 5

Conclusion

The aim of this paper was to model the coupled relationship between an energy harvesting civilization and their host planet, based on the assumption that the civilizations energy generation comes from some form of combustion. The work here builds off the work done in Frank et al., 2018, where they developed a simple analytic form of such a model to explore the idea that Anthropocenes might be a generic feature of any planet evolving a species that intensively harvests resources for the development of a technological civilization (Haqq-Misra and Baum, 2009; Frank, Alberti, and Keliedon, 2017; Mullan and Haqq-Misra, 2019). The principle innovation in this paper was the inclusion of a numerical climate model, allowing us to more realistically simulate planetary response to an evolving exocivilization. This model, called an Energy Balance Model (EBM), allowed us to investigate the effect that varying such planetary parameters as orbital distance and partial CO_2 pressure has on global temperatures. Furthermore, in contrast to (Frank et al., 2018), a different form for the population growth equation was also used.

Our equation for population growth was based on the logistic equation, so that initially it acted like exponential growth, with a "natural" growth rate based on our own, prior to the industrial revolution. In our model, we associated the civilizations technological capabilities with their production of combustion byproducts. As a result, increasing levels of pCO_2 acted to increase birth rates. As technology increased, the corresponding feedback raised global temperatures. This negative feedback was reflected in our equation for population growth by having increasing temperatures decrease the growth rate. Like the classic logistic equation, our version also had a carrying capacity, which acted to smoothly decrease the civilizations growth rate as they approached their maximum population. This ensured that our civilizations couldn't grow to levels that are unrealistic based purely on food production capabilities.

Using simulations of the coupled nonlinear model combined with semi-analytic treatments, we find that the majority of the planets in the CLHZ (Schwieterman et al., 2019; Ramirez, 2020) undergo a 'climate-dominated' Anthropocene. We have defined such an Anthropocene to occur when changes in climate occur on timescales that are short with respect to the populations own evolution. In other words, we say that an Anthropocene is 'climate-dominated' when the rate of climate change is faster than that for population growth. If a civilization experiences a climate-dominated Anthropocene, then they will begin to decline before reaching their carrying capacity. Thus, any civilization that does not reach their carrying capacity falls under our definition of experiencing a climate-dominated Anthropocene. We find that this occurs primarily on systems with high climate sensitivities (dT/dP), where small technological advancements can trigger massive climate change. Furthermore, as discussed in Section 3.1, we find that this is most likely to occur on planets with low levels of CO_2 in their atmosphere. Likewise, civilizations with low tolerances to temperature change (ΔT) are likely to experience such climate-dominated Anthropocenes irregardless of their orbital distance, as small deviations in their climate states could trigger massive extinction events.

Although, some civilizations are able to reach their carrying capacities before experiencing any dramatic climate change. Despite not falling under our definition of a climate-dominated Anthropocene, such civilization's should not be considered to have escaped the possibility of population collapse. These civilizations are said to have overpopulated their planet, which will inevitably lead to its own adverse outcomes. We find that such systems tend to have very low climate sensitivities and very high concentrations of CO_2. If we take Earth as an example, then that abundance of CO_2 could make such systems uninhabitable for the vast majority of complex aerobic life (Schwieterman et al., 2019), ensuring that climate-dominated Anthropocenes are a generic feature of any intelligent civilization.

Future work on this could focus on investigating the effect of energy harvesting by wind or solar. Alternatively, future efforts could explore different models for population growth and/or different methods of coupling such a model to the climate state. Other avenues for improvement could relate to considerations of the impact of various stellar spectral types, or our model could be modified to allow the civilizations to change their behavior, either by switching energy sources or limiting population growth. Doing so will allow further insights to be gained about the *astrobiology of the Anthropocene* by investigating issues associated with the biospheric aspects of sustaining long-term civilizations.

Appendices

Appendix A

Derivation of Collapse Time (τ_{coll})

A.1 Low Climate Forcing ($\gamma \ll 1$)

In this case, in order for $\beta \gg 1$, we require that $\theta \gg 1$. Thus, this implies that the technological timescale is less than the growth timescale which is less than the timescale for climate change. In this region of parameter space, models begin with exponentially rising populations. This is because at the start, we expect that $\eta \approx \epsilon \approx 0$, so that $\eta\epsilon^2 \approx 0$ and $1-\eta \approx 1$. It follows that at the start, $\eta(1+\theta\epsilon) < 1-\eta$ so that

$$\dot{\eta} = \eta(1+\theta\epsilon) - \eta\epsilon^2 \approx \eta$$

As population rises exponentially, eventually the carrying capacity is reached, at which point $\eta \approx 1$, $1-\eta \approx 0$, and $\eta\epsilon^2 \gtrapprox 1-\eta$. Thus...

$$\dot{\eta} = 1 - \eta - \eta\epsilon^2 \approx -\epsilon^2$$

This shows that when the carrying capacity is reached, the population will start to decline at a rate dictated by the environmental state, i.e. the global temperatures relative to their initial values. Also, since $\eta \approx 1$, we know that

$$\dot{\epsilon} = \gamma$$

Thus, the rate of population collapse is dictated by the environment, whose rate is dictated by γ. It follows that in this region the timescale for population collapse is

$$\tau_{\text{coll}} = \frac{1}{\dot{\epsilon}}\bigg|_{\eta=1} = 1/\gamma \qquad (\gamma \ll 1) \tag{A.1}$$

In other words, $\tau_{\text{coll}} = R_0 t_C$, where t_C is defined in Section 3.2.

It is of interest that this collapse time is independent of θ. This means that the increase in global CO_2 concentrations does not have a significant effect on the growth rate until after the population has peaked. After the population peaks, it begins to fall. As a result, $1-\eta$ is increasing while $\eta(1+\theta\epsilon)$ is decreasing. So initially after the collapse the birth rate is increasing. But, eventually their comes a point during the collapse when $1-\eta > \eta(1+\theta\epsilon)$, at which point the min function switches terms and as a result the birth rate begins to decrease, which has the effect of decreasing the overall growth rate and expediting the collapse. This switch between birth terms can be seen in the trajectories for these models as the dip in the slope of η during its decline, shown in Figure $A.1a$. For the models with higher θ, this dip occurs later since technology is able to increase the birth rate for a longer time.

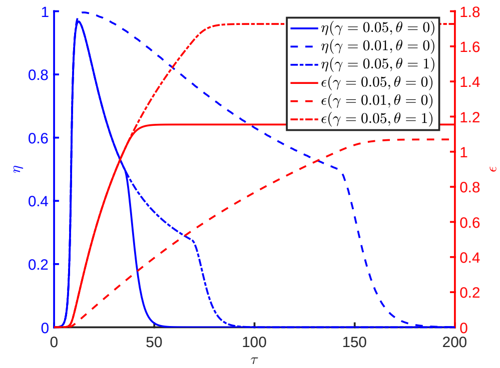

(a) Time Evolutions for Low Gamma

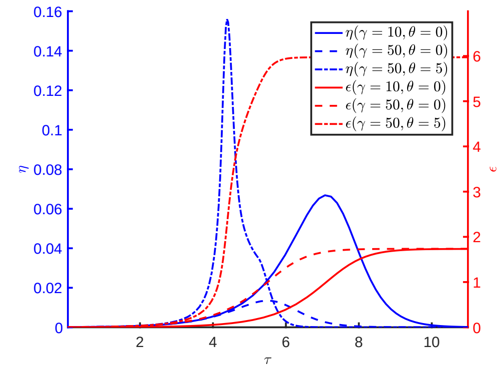

(b) Time Evolutions for High Gamma

Figure A.1: Trajectories of η/ϵ plotted against τ, found with the analytical model ($\alpha = 0$)

A.2 High Climate Forcing $(\gamma \gg 1)$

If $\gamma \gg 1$, then $t_C < t_G$, so the climate changes on a much faster rate than the population does. This is the region of the climate-dominated Anthropocene, which means that global temperatures will begin to increase death rates before civilizations reach their carrying capacity. A consequence of this is that civilizations in this region never reach their maximum growth rate or carrying capacity, $\eta \ll 1$, which implies that $1 - \eta > \eta(1 + \theta\epsilon)$, so their population growth equation will have the form.

$$\dot{\eta} = \eta(1 + \theta\epsilon) - \eta\epsilon^2 = \eta(1 + \theta\epsilon - \epsilon^2)$$

We can set $\dot{\eta} = 0$ and solve for ϵ to determine what the environmental state is at the point when population begins to collapse. We call this value of ϵ its critical value, which we find to be

$$\epsilon_c = \frac{\theta}{2} + \sqrt{1 + \left(\frac{\theta}{2}\right)^2} \quad (\dot{\eta} = 0)$$

We can also find the time scale for the population to decline after it reaches this peak. Since these civilizations do not reach their carrying capacity, their growth rate as they enter the Anthropocene dictates what their collapse rate will be directly after. Thus, we use the free fall time for civilizations as their collapse rate.

$$\tau_{\text{coll}} = \sqrt{-\frac{\eta}{\ddot{\eta}}}\Bigg|_{\dot{\eta}=0} \quad (\gamma \gg 1)$$

We can use our population growth rate equation to find this second derivative

$$\ddot{\eta} = \eta(\theta\dot{\epsilon} - 2\epsilon\dot{\epsilon}) = \eta\dot{\epsilon}(\theta - 2\epsilon)$$

When population begins to decline, global temperatures continue to rise exponentially. Thus, at this point, the rate of increasing temperatures is approximately equal to its critical value.

$$\dot{\epsilon_c} = \epsilon_c \quad (\dot{\eta} = 0)$$

Thus, it follows that at this point, directly after $\dot{\eta} = 0$...

$$-\ddot{\eta} \approx \eta(2\epsilon_c^2 - \theta\epsilon_c) \quad (\dot{\eta} = 0)$$

Thus, it follows that the collapse timescale for $\gamma \gg 1$ is given by

$$\tau_{\text{coll}} = \left(2\epsilon_c^2 - \theta\epsilon_c\right)^{-1/2} \quad (\gamma \gg 1)$$

This can further be broken down into two cases, dependent on θ.

Low Technological Growth Acceleration ($\theta \ll 1$)

In this case, the civilizations technological abilities are not advanced enough to increase their growth rates. Also, the fastest timescale is that for climate change. Since their rate of technological advancements is negligible and their rate of climate change exceeds that for population growth, these civilizations will have negligible population growth before entering their Anthropocene. As a result, their growth rate as they enter the Anthropocene will be approximately equal to its initial "natural" value. Thus, all civilizations in this area will also collapse with a constant "natural" collapse rate. Specifically, if $\theta \ll 1$, then $\epsilon_c \approx 1$ and

$$\tau_{\text{coll}} = \frac{1}{\sqrt{2}}$$

High Technological Growth Acceleration ($\theta \gg 1$)

In this case the civilizations technological abilities are able to accelerate their growth rates. Thus, these civilizations enter their Anthropocene with an accelerated growth rate due to their technological abilities. This accelerated growth leads to an accelerated decline, which means that these civilizations collapse at a faster than natural rate. Specifically, if $\theta \gg 1$, then $\epsilon_c \approx \theta$ and

$$\tau_{\text{coll}} = \frac{1}{\theta}$$

To be more precise, civilizations with high γ and θ will initially have $\eta \approx \epsilon \approx 0$, which like the case of low gamma means that $1 - \eta > \eta(1 + \theta\epsilon)$. As a result, at the beginning $\dot{\eta} = \eta(1 + \theta\epsilon - \epsilon^2)$, so technology has the effect of enhancing the birth rate, allowing the civilization to grow at a faster than natural rate. The min function ensures that this rate doesn't reach unrealistic values by setting a maximum growth rate. Once the technology-enhanced growth rate reaches this limit, the min function switches birth terms so that the civilization can head smoothly into the decline with $\dot{\eta} = 1 - \eta - \eta\epsilon^2$. At this point η begins to decrease so $1 - \eta$ starts to increase. Eventually, we reach the state we started at where $1 - \eta > \eta(1 + \theta\epsilon)$. The min function again switches terms, so that the birth rate switches from its maximum value to its technology-enhanced value. This has the effect of softening the decline, and can be seen during the collapse of the trajectory with $\gamma = 50$, $\theta = 5$ in Figure $A.1b$ as a slight deviation in the slope of η.

Appendix B

Effective Climate Forcing (γ_{eff})

The value of γ we defined in Section 3.3 is based on the initial value of the planets climate state (when $T = T_0$ and $P = P_0$). More specifically, it is based on the initial value of the planets climate sensitivity, thus has the form

$$\gamma = \left(\frac{CN_{max}}{R_0 \Delta T}\right) \frac{dT}{dP}\bigg|_{T_0} \equiv \frac{DCN_{max}}{R_0 \Delta T}$$

This quantity describes the likelihood that a planets initial state will trigger a climate-dominated Anthropocene. Likewise, we can define an 'effective' γ, that will describe this likelihood when the planet has reached its peak population, which occurs approximately when global temperatures have increased by ΔT. Thus, this will have the form

$$\gamma_{\text{eff}} = \left(\frac{CN_{max}}{R_0 \Delta T}\right) \frac{dT}{dP}\bigg|_{T_0+\Delta T} \equiv \left(\frac{DCN_{max}}{R_0 \Delta T}\right) e^{-\Delta T/\Delta T_F} \tag{B.1}$$

Comparing this with our equation for γ and using our definition for α as defined in Section 3.4.1 ($\alpha \equiv \Delta T/\Delta T_F$), we find that

$$\boxed{\gamma_{\text{eff}} = \gamma e^{-\alpha} \geq \gamma} \tag{B.2}$$

Figure B.1 shows the effect that this has on the models as a 4×4 grid. The top left plot shows our numerically calculated values of γ, as defined in Table 3.1 and derived in Section 3.3, plotted versus the numerically calculated times for our models populations to decline by 20% from their peak values. The black dotted line shows our analytical expression for the collapse time, derived in Section 3.5. For contrast, the bottom left plot shows the same things yet instead for γ_{eff}, as given by Eq. B.1. The biggest difference as compared to the plot above is a net decrease in γ, which is as expected from Eq. B.2. This also has the effect of greatly reducing the deviations from our analytical predictions, i.e. adheres much more to our check-mark shaped prediction (see Fig. 3.2).

Although, not all deviations have been solved by using γ_{eff}. The right column of Figure B.1 shows plots of γ_{eff} colored by orbital distance (top-right), and initial global temperature (bottom-right). It can be seen that the models that deviate greatest from our analytical prediction are those that have large orbital radii and low initial global temperatures. As shown in Figure 4.3, the contour lines for pCO_2 travel diagonally across the parameter space of a/T_0. Thus, as a result, civilizations with high orbital distance and low initial global temperature could have the same value of initial pCO_2 as the civilizations with low orbital distance and high initial global temperature. Since γ is principally dependent on the value of initial pCO_2, this means that these two classes of civilizations will have the same value of γ and hence the same value of τ_{coll}. Although, in reality, the civilizations with the higher orbital radii end up taking longer to fall, hence have longer decline times.

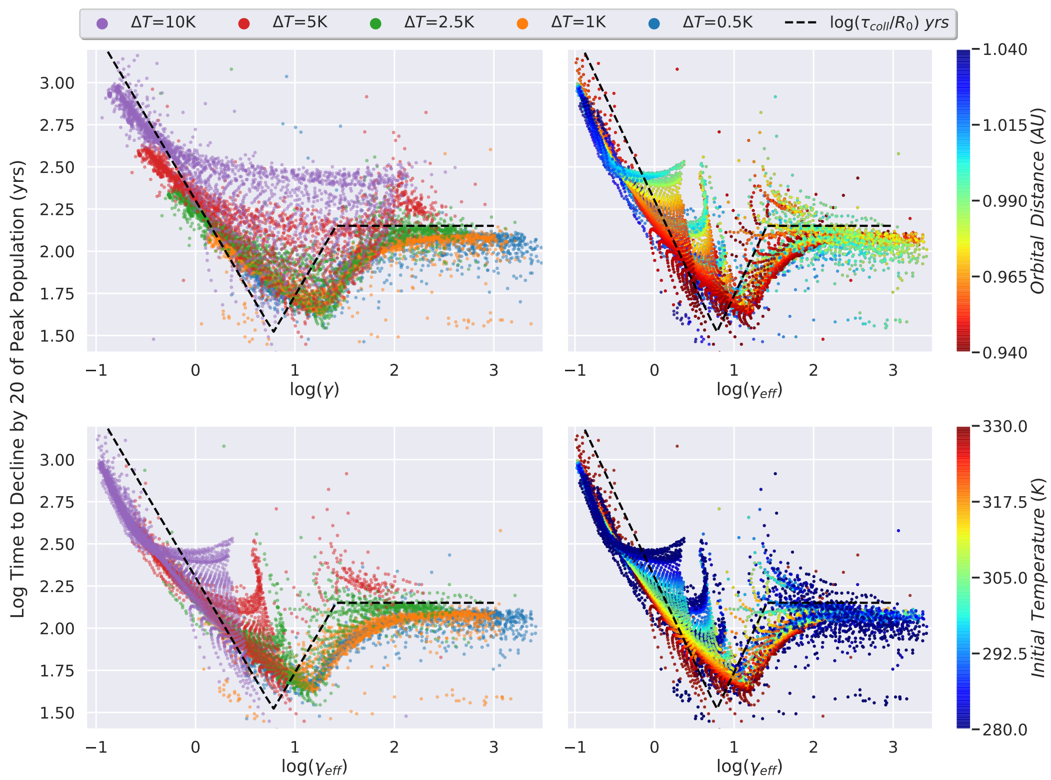

Figure B.1: The top left plot shows our numerically calculated values of γ. For contrast, the bottom left plot shows the same things yet instead for γ_{eff}, as given by Eq. B.1. The biggest difference as compared to the plot above is a net decrease in γ, which is as expected from Eq. B.2. This also has the effect of greatly reducing the deviations from our analytical predictions, that is, adheres much more to our check-mark shaped prediction. Although, not all deviations have been solved by using γ_{eff}. The right column shows plots of γ_{eff} colored by orbital distance (top-right), and initial global temperature (bottom-right). It can be seen that the models that deviate greatest from our analytical prediction are those that have large orbital radii and low initial global temperatures.

Bibliography

Carroll-Nellenback, J. et al. (2019). “The Fermi Paradox and the Aurora Effect: Exo-civilization Settlement, Expansion, and Steady States”. In: *The Astronomical Journal* 158. DOI: 10.3847/1538-3881/ab31a3.

Catling, D. C. et al. (2005). “Why O_2 Is Required by Complex Life on Habitable Planets and the Concept of Planetary “Oxygenation Time””. In: *Astrobiology* 5, pp. 415–438. DOI: 10.1089/ast.2005.5.415.

Crutzen, P. J. (2002). “The “anthropocene””. In: *Journal de Physique IV* 12, pp. 1–5. DOI: 10.1051/jp4:20020447.

Elhacham, E., L. Ben-Uri, J. Grozovski, et al. (2020). “Global human-made mass exceeds all living biomass”. In: *Nature* 588, pp. 442–444. URL: https://doi.org/10.1038/s41586-020-3010-5.

Fairen, A. G., J. D. Haqq-Misra, and C. P. (2012). “Reduced albedo on early Mars does not solve the climate paradox under a faint young Sun =”. In: *EDP Sciences 540* A13. URL: https://doi.org/10.1051/0004-6361/201118527.

Frank, A., M. Alberti, and A. Keliedon (2017). “Earth as a Hybrid Planet, The Anthropocene in an Evolutionary Astrobiological Context, Anthropocene, (in press)”.

Frank, A. et al. (2018). “The Anthropocene Generalized: Evolution of Exo-Civilizations and Their Planetary Feedback”. In: *Astrobiology* 18, pp. 503–518. DOI: 10.1089/ast.2017.1671.

Haqq-Misra, J. D. and S. D. Baum (2009). “The Sustainability Solution To The Fermi Paradox”. In: *Journal of the British Interplanetary Society* 62, pp. 47–51.

Huang, Y. and M. Bani Shahabadi (2014). “Why logarithmic? A note on the dependence of radiative forcing on gas concentration”. In: *J Geophys. Res. Atmos.* 119.13, pp. 683–13, 689. DOI: 10.1002/2014JD022466.

IPCC (2014). “Synthesis Report”. In: *Contribution of Working Groups I, II and III to the Fifth Assessment Report of the Intergovernmental Panel on Climate Change*. Ed. by R. K. Pachauri Core Writing Team and L. A. Meyer (eds.) Geneva, Switzerland: IPCC, p. 43.

Kuehn C., Physica D (2011). *A mathematical framework for critical transitions: Bifurcations, fast-slow systems and stochastic dynamics”*. 240th ed.

Lenton, T. et al. (2008). “Tipping elements in the Earth’s climate system”. In: *PNAS* 105, pp. 1786–1793.

Mullan, B. and J. Haqq-Misra (2019). “Population growth, energy use, and the implications for the search for extraterrestrial intelligence”. In: *Futures* 106, pp. 4–17. DOI: 10.1016/j.futures.2018.06.009.

North, G. and K. Kim (2017). *Energy Balance Climate Models*. New York: Wiley.

Ramirez, R. M. (2020). "A Complex Life Habitable Zone Based On Lipid Solubility Theory". In: *Scientific Reports* 10. DOI: 10.1038/s41598-020-64436-z.

Savitch, Ethan et al. (2021). *Triggering A Climate Change Dominated "Anthropocene": Is It Common Among Exocivilizations?* arXiv: 2103.06330 [astro-ph.EP].

Schwieterman, E. W. et al. (2019). "A Limited Habitable Zone for Complex Life". In: *The Astrophysical Journal* 878. DOI: 10.3847/1538-4357/ab1d52.

Solomon, S. et al. (2007). *Climate Change 2007: The Physical Science Basis*. Cambridge, United Kingdom and New York, NY, USA: Cambridge University Press.

Williams, Darren M. and James F. Kasting (1997). "Habitable Planets with High Obliquities". In: *Icarus* 129.1, pp. 254–267.

Wittmann, A. C. and H.-O. Pörtner (2013). "Sensitivities of extant animal taxa to ocean acidification". In: *NatCC* 3, p. 995.